

# Mathematical Study of the Effects of Different Intrahepatic Cooling on Thermal Ablation Zones

Tingying Peng\*, David O'Neill, Stephen Payne (\*tingying.peng@eng.ox.ac.uk)

Institute of Biomedical Engineering, Department of Engineering Science, University of Oxford, UK

**Abstract**— Thermal ablation of a tumour in the liver with Radio Frequency energy can be accomplished by using a probe inserted into the tissue under the guidance of medical imaging. The extent of ablation can be significantly affected by heat loss due to the high blood perfusion in the liver, especially when the tumour is located close to large vessels. A mathematical model is thus presented here to investigate the heat sinking effects of large vessels, combining a 3D two-equation coupled bio-heat model and a 1D model of convective heat transport across the blood vessel surface. The model simulation is able to recover the experimentally observed different intrahepatic cooling on thermal ablation zones: hepatic veins showed a focal indentation whereas portal veins showed broad flattening of the ablation zones. Moreover, this study also illustrates that this shape derivation can largely be attributed to the temperature variations between the microvascular branches of portal vein as compared with hepatic vein. In contrast, different amount of surface heat convection on the vessel wall between these two types of veins, however, has a minor effect.

## I. INTRODUCTION

RADIO Frequency Ablation (RFA) has been widely used for the treatment of focal primary and secondary liver malignancies as a minimally invasive, image-guided alternative to standard surgical resection ([1]). An EU-funded research project, IMPACT, has been initiated to develop an intervention planning system for RFA that is able to simulate the electric-thermal heating processes during the ablation procedure and to predict the lesion zone after the ablation. The classical bio-heat equation, Pennes model, has been widely used in the literature to model the heat sink effect of blood flow ([2]). It assumes that the blood is delivered to each capillary at a constant arterial blood temperature and reaches equilibrium with the surrounding tissue before it is removed by the veins, which no longer influence the tissue temperature. Some shortcomings in the Pennes model are due to its inherent simplicity, as pointed out by Wulff [3]: it assumes a uniform perfusion rate without accounting for the blood flow direction and chooses only the venous blood stream as the fluid stream equilibrated with the tissue. Due to the absence of an equation to model the blood temperature variation, large deviations have been found between Pennes model predictions and the absolute temperature field in a vascularized tissue [4-5]. Therefore, we have developed a new mathematical model of a two-equation coupled system to include the effect of directional blood perfusion [6], as part of the IMPACT project.

The new bio-heat model breaks an arbitrary control volume down to two subvolumes: tissue and blood, and sets up one bio-heat equation for each volume, similar to the approach of [7]. Heat is convectively transferred between the two subvolumes, making the two equations coupled. Unlike the previous model of Klinger [8], local thermal equilibrium between tissue and blood temperature was not assumed. Analytical analysis and numerical simulations have shown that this new model is equivalent to the classical Pennes model and Klinger model when estimating the cooling effects of large vessels (such as big arteries and veins) and very small vessels (such as arterioles, venules and capillaries), respectively [6]. However, the majority of the vasculature cooling is attributed to the vessels of median sizes such as terminal vessel branches, in which case the two-equation model provides a better estimation [6].

This paper, therefore, utilises this model to simulate the dynamics of tissue temperature in the presence of two large blood vessels (>3mm) during RFA: one portal vein (PV) supplying blood into tissue and one hepatic vein (HV) draining blood out. These two types of liver vessels are modelled separately because of their different volume and shape alterations of the ablation zones, as reported in [9]. The effect of blood flow perfusion on tissue temperature distribution dynamics consists of (a) convective heat exchange at wall surface of the large vessel and (b) cooling effects of small vessels branched from this large vessel. This paper illustrates that (b) is the main physical mechanism leading to the experimentally observed different cooling effects between portal field and hepatic veins, though it has not been investigated as intensively as (a) in the literature.

## II. METHODS

### A. Mathematical model

The dynamic temperature distribution was modelled in a cube of tissue in which two large vessels are located, as shown in Figure 1. The temperature distribution dynamics in the tissue are represented by two temperatures:  $T_t$ , the temperature of a solid tissue subvolume, and  $T_b$ , the temperature of the blood subvolume, given by the following coupled bio-heat equations:

$$\rho_t c_t \frac{\partial T_t}{\partial t} = q_t + \nabla \cdot (k_t \nabla T_t) - \frac{H_{tb}}{1-\phi} (T_t - T_b) \quad 1(a)$$

$$\rho_b c_b \frac{\partial T_b}{\partial t} = q_b + \nabla \cdot (k_b \nabla T_b) + \frac{H_{tb}}{\phi} (T_t - T_b) - \rho_b c_b (\vec{u}_b \cdot \nabla T_b) \quad 1(b)$$

where  $\rho_t$ ,  $\rho_b$ ,  $c_t$ ,  $c_b$ ,  $k_t$ ,  $k_b$ ,  $H_{tb}$ ,  $\phi$ ,  $q_t$  and  $q_b$  are tissue density, blood density, tissue specific heat capacity, blood specific heat capacity, tissue thermal conductivity, blood thermal conductivity, local volumetric heat transfer

Manuscript received June 14, 2011. This work was supported by European Community's Seventh Framework Programme under Grant n22877, project IMPACT.

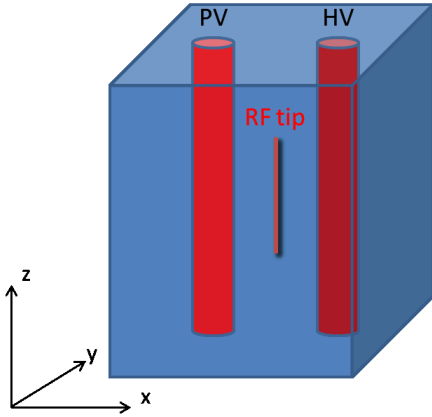


**Figure 1: Model schematic.** The numerical simulation domain is a cube of tissue ( $50 \times 50 \times 50 \text{mm}^3$ ) with a grid size of 1mm in each direction. RF electrode (1cm length, 0.5mm diameter) is placed along the central line of the cube. One portal vein (PV) and one hepatic vein (HV) (both of 3mm diameter) are placed symmetrically in the cube.

coefficient, blood volume fraction, blood flow velocity, tissue RF power deposition and blood RF power deposition, respectively.

Within the tissue region to be ablated, a vessel with a diameter of more than 3 mm ([10]) close to the tumour can have a significant effect on heat loss. The average blood temperature within the vessel is considered as a continuous function  $T_f(z)$  of axial position  $z$  only, with the assumption of quasi-equilibrium when the blood velocity satisfies  $\frac{\partial T_f}{\partial t} \ll u_z \frac{\partial T_f}{\partial z}$ . The convective heat exchange at the vessel wall (for both PV and HV) is:

$$\rho_b c_b (\pi R^2) u_z \frac{\partial T_f}{\partial z} = h_c \cdot 2\pi R (T_t|_w - T_f), \quad h_c = \frac{Nu \cdot k_b}{2R}, \quad (2)$$

where  $R$  is the vessel radius,  $u_z$  is the blood flow velocity in the vessel,  $T_t|_w$  is the tissue wall temperature, and  $Nu$  is the Nusselt number. Despite the comparable vessel sizes, the flow velocities within the hepatic veins are significantly lower than within the portal fields [9]. As a result,  $u_z$  in the HV is set to be half of the amount in the PV in the simulation, though their radii are assumed to be the same:

$$u_z|_{PV} = V, \quad u_z|_{HV} = V/2.$$

Since the thickness of the vessel wall is very thin ( $< 0.5 \text{mm}$ ) compared to a large vessel diameter (5-10mm) ([9]), this convective heat transfer will be balanced by the conductive heat transfer on the tissue:

$$-k_t \frac{\partial T_t}{\partial r} \Big|_w = \frac{Nu \cdot k_b}{2R} (T_t|_w - T_f) \quad (3)$$

Equation (2) and (3) provide a thermal boundary condition for tissue temperature of porous media. The boundary for blood temperature of porous media is given by:

$$T_b|_w = T_f$$

So far, the coupled bio-heat transfer equation can still not be solved without the preliminary knowledge of blood

flow velocity  $\vec{u}_b$  in equation 1(b). Darcy's law suggests that the flow velocity is the gradient of pressure:

$$\vec{u}_b = -\frac{\kappa}{\mu \phi^3} \nabla p, \quad (4)$$

in which the pressure value can be evaluated using Laplace's equation based on continuity of blood flow velocity:

$$\nabla \cdot \vec{u}_b = \nabla \cdot \left( -\frac{\kappa}{\mu \phi^3} \nabla p \right) = 0. \quad (5)$$

$\vec{u}_b$  is the averaged blood flow velocity of all branches from the major vessel (assuming that 20% of the total blood in the major vessel goes to the branches in the tissue cube). As the PV supplies blood to the tissue whereas the HV drains blood out, the boundary conditions of  $\vec{u}_b$  are given as:

$$\vec{u}_b|_{PV} = \frac{\pi R^2 u_z|_{PV} \cdot 20\%}{2\pi RL} \hat{r}_p = \frac{RV}{10L} \hat{r}_p \quad (6a)$$

$$\vec{u}_b|_{HV} = -\frac{\pi R^2 u_z|_{HV} \cdot 20\%}{2\pi RL} \hat{r}_h = -\frac{RV}{20L} \hat{r}_h \quad (6b)$$

in which  $\hat{r}_p$  and  $\hat{r}_h$  are unit vectors of the radial directions of PV and HV, respectively;  $L$  is the length of the vessel in the tissue cube.

### B. Numerical and Computer Simulation Methods

The finite difference method was used to numerically solve the Laplace equation of pressure (thus flow velocity  $\vec{u}_b$ ). With the flow velocity field, partial differential equations in the thermal model (Eq. (1)) can be accurately solved by a standard finite difference method, Crank-Nicolson method, with suitable time (20s) and spatial step size (1mm).

As shown in Figure 1, a RF tip was placed between the two vessels to deliver RF power for ten minutes. The RF electrode probe is monopolar and can be considered as a uniform line source, with the heat source distribution  $q(r, t)$  varying inversely with the square of the distance from the RF electrode probe,  $r - r_p$  [11-12]:

$$q(r, t) = \frac{h_p}{[r - r_p]^2}, \quad r > r_p. \quad (7)$$

$$q_t = (1 - \phi)q, \quad q_b = \phi q$$

Since the radius of the RF electrode probe (0.25mm) is much smaller than the grid size used in the simulation, the heat source distribution in the voxel containing the probe is calculated by assuming  $r - r_p = \Delta l/2$ , which prevents a singularity in  $q$ . The constant  $h_p$  is determined by setting the total power deposited by the probe to be 5W.

Both the portal vein and hepatic vein (3mm in diameter) were assumed to be 8mm away from the centre of RF tips. The diameter value of the large vessel is taken from the typical size of a large vessel in a human liver [10]. The distance of 8 mm was chosen to be at the border of a lesion radius of interest, which is about 10 mm.

The values of the parameters associated with the thermal model were taken from previous studies [6], and are summarized in Table 1.

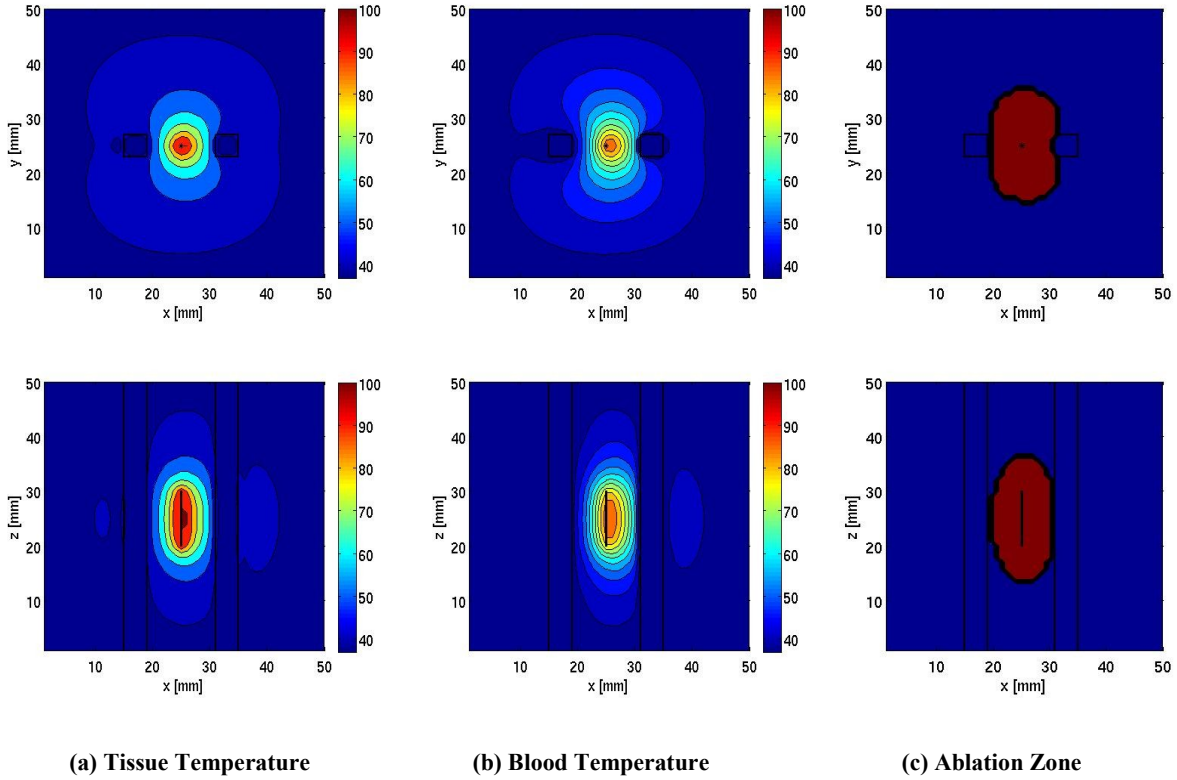


**Figure 2: Two-equation coupled model predictions, includes isothermal contours (in °C) in tissue (a) and blood (b) at the end of the ablation procedure and the corresponding lesion zone (c). Top figures: plan view; Bottom figures: vertical view. The PV is located on the left side whereas the HV is located on the right side in all figures (indicated by the back square or column).**

**Table 1 Model parameters**

Parameter and Description	Value and Unit
$\rho_t$ , tissue density	1060 $kgm^{-3}$
$\rho_b$ , blood density	1060 $kgm^{-3}$
$c_t$ , tissue specific heat capacity	3600 $Jkg^{-1}K^{-1}$
$c_b$ , blood specific heat capacity	4180 $Jkg^{-1}K^{-1}$
$k_t$ , tissue thermal conductivity	0.49 $WJm^{-1}K^{-1}$
$k_b$ , blood thermal conductivity	0.49 $WJm^{-1}K^{-1}$
$\phi$ , blood volume fraction	0.1
$H_{tb}$ , volume-averaged heat transfer coefficient	5000 $Wm^{-3}K^{-1}$
$V$ , blood flow velocity in portal vein	0.106 $ms^{-1}$
$h_p$ , RF power deposition coefficient	8.01 $Wm^{-1}$

### III. RESULTS AND DISCUSSION

The spatial tissue and blood temperature distributions at the end of the ablation procedure are shown in Figure 2(a) and (b), respectively. Both large vessels have demonstrated strong vessel cooling effects, suggested by the low temperature zone surrounding the vessel ( $<50^\circ C$ ). The tissue and blood thermal field are both non-symmetric, which reflects the directional cooling effects of the blood flow. The corresponding lesion zone takes  $50^\circ C$  isothermal contours of the tissue temperature as a threshold. The vessel cooling reveals a strong dependence on the vessel type: HV shows a focal indentation of the ablation zone whereas PV shows a

broad flattening effect (Figure 2(c), top figure). This agrees well with the experimental observed shape deviations between the ablation zones influenced by PVs as compared with HVs [9].

Though the model is able to recover the experimentally observed features, the underlying mechanisms for the different effects of HV and PV on thermal ablation zones are still not explicit. Two potential factors contribute to this derivation: (a) different amount of convective heat transfer (due to different velocities within PV and HV); (b) the blood in the vessel branches of PV remains cold while it has been heated up in the vessel branches of HV. Factor (a) is now evaluated independently by replacing the vessel branch (modelled as porous flow) cooling with the conventional homogenous heat sink as the Pennes model. Figure 3 shows the predicted tissue spatial temperature distribution and the lesion zone. The thermal field is found to be mostly symmetric, with only a small difference between the two vessel wall temperatures ( $<0.1^\circ C$ ), as a result of different flow velocities in PV and HV. The predicted lesion zone suggests that both PV and HV show a focal indentation effect, which does not agree with the experimental observations. This ruled out the factor (a) as a main factor for the different cooling effect of PV and HV. Instead, it is suggested that the microvascular branches (factor (b)) are the major physical mechanism contributing to the experimentally observed PV/HV derivation.

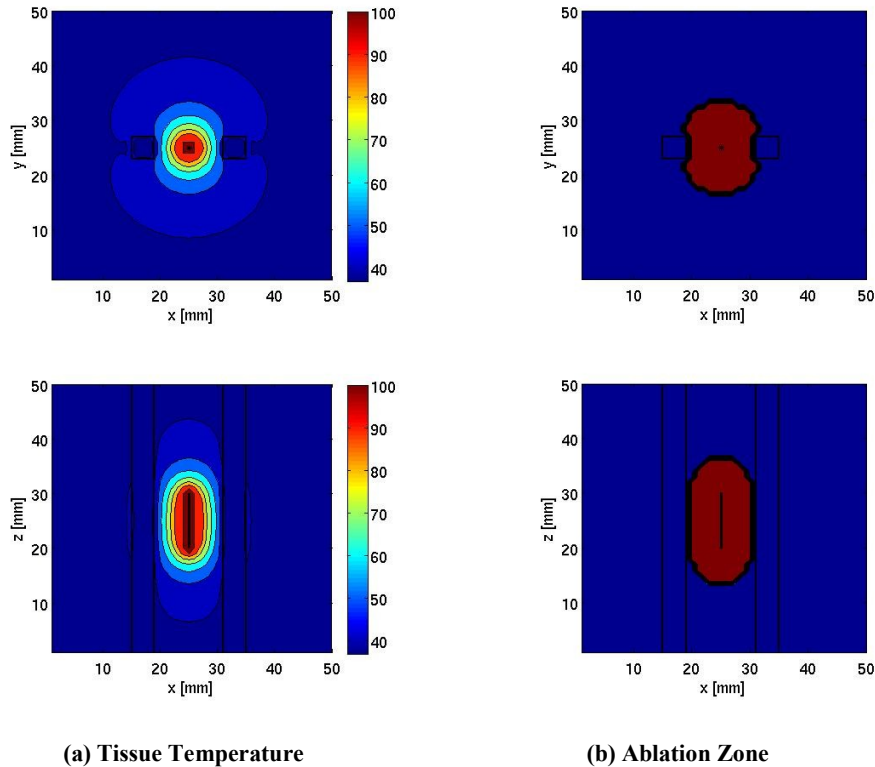


**Figure 3: Pennes model predictions, includes isothermal contours (in °C) in tissue at the end of the ablation procedure (a) and the corresponding lesion zone (b). Top figures: plan view; Bottom figures: vertical view. The PV is located on the left side whereas the HV is located on the right side in all figures (indicated by the back square or column).**

#### IV. CONCLUSION

This study has modelled the process of thermal ablation in tissue surrounding two large vessels (one PV supplying the blood into the tissue and one HV draining the blood out). The heat sinking effect of each large vessel has been divided into two parts: (a) convective heat exchange at vessel surface; (b) its small vessel branches modelled as porous media flow cooling. The model simulation suggests that the experimentally observed different shape alterations of PV and HV on the ablation zone is largely due to the different blood temperatures in the microvascular branches of PV and HV (factor (b)), whilst the different amount of convective heat exchange due to different flow velocities within PV and HV (factor (a)) play only a minor role. These different cooling effects of PV and HV may have important clinical implications for thermal ablation treatment and have to be taken into consideration when planning such procedures.

#### REFERENCES

- [1] E.J. Berjano, "Theoretical modeling for radiofrequency ablation: state-of-the-art and challenges for the future". *Biomed Eng OnLine*, Vol 5, 2006.
- [2] H. H. Pennes "Analysis of tissue and arterial blood temperatures in the resting human forearm," *J Appl Physiol*, vol. 85, no. 1, pp. 5–34, July 1998.
- [3] W. Wulff, "The Energy conservation equation for living tissue", *Biomed. Eng. IEEE Trans.* Vol. 21, no. 6, pp. 494-495, 1974.

- [4] H. Brinck, and J. Werner, "Efficiency function: improvement of classical bioheat approach", *J. Appl. Physiol.* Vol. 77, no. 4, pp 1617–1622, 1994.
- [5] H. Brinck and J. Werner, "Use of vascular and non-vascular models for the assessment of temperature distribution during induced hyperthermia", *International Journal of Hyperthermia: the Official Journal of European Society for Hyperthermic Oncology*, North American Hyperthermia Group, Vol. 11, No. 5, pp. 615–626, 1995.
- [6] T. Peng, D. P. O'Neill and S. J. Payne, "A two-equation coupled system for determination of liver tissue temperature during thermal ablation", *Int. J. Heat Mass Transfer*, Vol. 54, pp. 2100-2109, 2011.
- [7] M. M. Chen and K. R. Holmes, "Microvascular contributions in tissue heat transfer." *Annals of the New York Academy of Sciences*, vol. 335, pp. 137–150, 1980.
- [8] H. Klinger, "Heat transfer in perfused biological tissue I: general theory", *Bull. Math. Biol.* Vol. 36, No. 4, pp. 403–415, 1974.
- [9] B. B. Frericks, J. P. Ritz, T. Albrecht, S. Valdeig, A. Schenk, K. Wolf and K. Lehmann, "Influence of intrahepatic vessels on volume and shape of percutaneous thermal ablation zones", *Investigative Radiology*, Vol. 43, No. 4, April 2008.
- [10] A. Galea and R. Howe, "Liver Vessel Parameter Estimation From Tactile Imaging Information," in *Proceedings of Medical Simulation: International Symposium-ISMS 2004*, pp. 59-66, 2004.
- [11] X. Chen and G. Saidel, "Mathematical modeling of thermal ablation in tissue surrounding a large vessel", *J. Biomech. Eng.* Vol. 131, No. 1, pp. 011001, 2009.
- [12] X. Chen, K. Barkauskas, S. Nour, J. Duerk, F. Abdul-Karim and G. Saidel, "Magnetic resonance imaging and model prediction for thermal ablation of tissue", *J. Magn. Reson. Imaging* Vol. 26 No. 1, pp. 123–132, 2007